

Macroscopic and microscopic model analysis of polarized protons scattering on ^{18}O

J. L. Escudié, R. Lombard, M. Pignanelli,* F. Resmini,* and A. Tarrats

DPh-N/ME, CEN Saclay, BP 2, 91190 Gif-sur-Yvette, France

(Received 5 November 1973)

Differential cross sections and analyzing powers for polarized (p, p') scattering on ^{18}O have been measured at an incident proton energy of 24.5 MeV, using the Saclay AVF cyclotron. Data have been taken for nine levels, up to 7.11 MeV excitation energy. The analysis has been carried out in the distorted wave Born approximation within the framework of the macroscopic and microscopic models. For the latter the available wave functions of ^{18}O and an approximate description of the nucleon-nucleon interaction, derived from the Hamada-Johnston potential, have been used. The macroscopic model, with just a simple deformation parameter β , accounts reasonably well for some even-parity transitions, and also for the excitation of the 3^- level at 5.09 MeV. Furthermore, coupled-channel calculations support evidence for a rotational band based on the ground state and including the 2^+ at 1.98 MeV and the 4^+ at 7.11 MeV. The analysis also supports a collective character of the 3^- level at 5.09 MeV and accounts for the observed strong excitation of this state. Satisfactory fits are obtained for some levels within the microscopic model, even though the absolute values of the cross sections are usually underestimated and large normalization factors needed. The use of an imaginary form factor adds some structure to the calculated angular distributions and improves the agreement between theory and experiment for those transitions for which the real form factor is collectivelike, i.e., peaked at the nuclear surface.

[NUCLEAR REACTIONS $^{18}\text{O}(p, p')^{18}\text{O}$, $E = 24.5$ MeV; measured $\sigma(\theta)$ and analyzing power for nine levels. Macroscopic and microscopic DWBA calculations.]

I. INTRODUCTION

Inelastic scattering of protons has been widely used as a tool for investigating both collective and microscopic aspects of the nuclear structure. Especially in this second case related to the recent developments of microscopic models,¹⁻³ the availability of more realistic sets of wave functions and nucleon-nucleon interactions has contributed much to a progressive understanding of the experimental data.

The use of polarized proton beams has turned out as useful, since analyzing power data have helped both in clarifying the role of the spin-orbit term within macroscopic models,⁴⁻⁶ and removing ambiguities from the optical model analysis of elastic scattering.^{7,8} The understanding of the real importance of the spin-orbit term in the microscopic description of inelastic scattering is still in its early stage,⁹⁻¹² although there is evidence that it should not be neglected as was the case in early studies.¹³

In this respect, light nuclei in the $1p$ and $2s-1d$ shells seem to offer a fair chance to study the reaction mechanisms and to test the existing models.

In this paper we present the results of an inelastic proton scattering experiment with a polarized proton beam of 24.5 MeV on ^{18}O , where data have been taken on most states up to an excitation energy of 8 MeV.

Several papers have been recently published on the level structure of ^{18}O , since some low-lying positive parity states are not accounted for by the simple shell model picture of two neutrons outside the ^{16}O core. The $2p-0h$ configurations give rise to $J=0^+$, 2^+ , 4^+ states of the $(1d_{5/2})^2$ type, $J=0^+$ [$(2s_{1/2})^2$] and $J=2^+$, 3^+ [$(1d_{5/2}, 2s_{1/2})$]. Other states not explained by this scheme are a 2^+ state at 5.25 MeV and a 0^+ state at 5.35 MeV. Admixtures of simple shell model and collective states have therefore been considered by various authors,¹⁴⁻¹⁹ with explicit calculations of the wave functions of low-lying 0^+ and 2^+ states. Sometimes rather different results have been obtained, but the presence of collective components, or $4p-2h$ states, is fairly well established.

Previously unpolarized proton scattering data on ^{18}O have been reported by Stevens, Lutz, and Eccles²⁰ for incident energies up to 16.3 MeV and for the transitions to the ground state and to the first 2^+ excited state. The aim of the present experiment was therefore to get analyzing power data at higher energies in order to reduce compound nucleus contributions and to study the transitions up to the 4^+ state at 7.11 MeV. The purpose was to investigate the collective and microscopic structure of these levels and the associated reaction mechanism for exciting these states.

Calculations have been made using both macroscopic and microscopic models. A previous col-

lective model analysis concerning only the 0^+ (g.s.), 2^+ state at 1.98 MeV, and 4^+ state at 7.11 MeV which yielded evidence for a rotational band based on the ground state and allowed a measurement of the β_2 and β_4 values, has been reported elsewhere.²¹

Microscopic calculations were performed using a complete nucleon-nucleon ($N-N$) interaction derived from the Hamada-Johnston potential²² and including spin-orbit and tensor terms. Imaginary form factors were introduced in some calculations to simulate both the presence of an imaginary component in the effective ($N-N$) interaction, as suggested by Satchler²³ and nondirect reaction mechanisms. The wave functions used were those of Zuker,²⁴ and in a few cases also those of Engel- and.¹⁶

II. EXPERIMENT

Differential cross sections and analyzing powers were measured using the polarized proton beam of the Saclay AVF cyclotron at an incident energy of 24.5 MeV. Data on elastic scattering were taken also at 22.5 MeV, in order to ensure that large compound nucleus contributions would not hamper the optical model analysis.

The 98% pure ^{18}O isotope was contained in a cylindrical gas cell of 3 cm diam, with entry and exit windows covered by 2 mg/cm² thick Havar foils. The target was run at a pressure of 0.5 atm and the pressure was continuously monitored with a high precision dial manometer. A thermometer provided a control of the target temperature.

The scattered particles were detected with an array of 16 Si(Li) detectors, 4 mm thick, cooled to approximately -20° with a circulating freon system. The collimator system in front of each detector consisted of two slits. One, at a distance

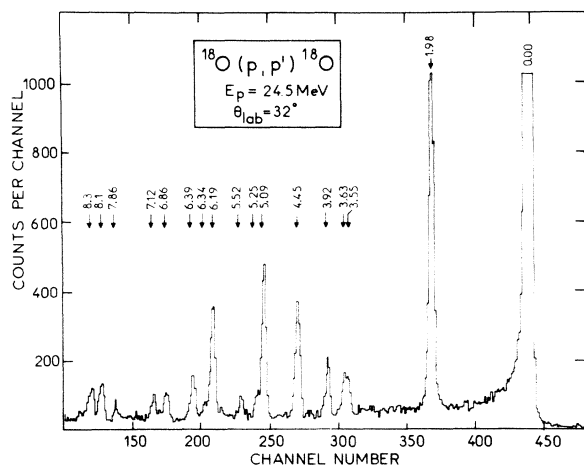


FIG. 1. Typical spectrum taken at 32° laboratory angle.

of 79 mm from the center of the target, was a 1 mm wide tantalum slit. The second, at 144 mm from the target, was a rectangular tantalum collimator 1 mm wide and 8 mm tall. The resulting angular resolution was about 0.8° . The over-all energy resolution, including the kinematical spread, was between 80 and 100 keV for all counters.

Data were taken every 5° , from 20 to 165° laboratory angles, and events were recorded with an on-line CAE 90 10 computer. The beam polarization was periodically reversed during the run, at a frequency of 5 Hz, and it was continuously monitored with a carbon polarimeter, whose details are given elsewhere.²⁵ The average beam polarization was about 85%, and the typical beam current on target between 8 and 10 nA. A typical spectrum is shown in Fig. 1. Several spectra at the same angle were summed and then unfolded in order to resolve the close levels.

Differential cross sections and analyzing powers were measured for the levels at 1.98 MeV (2^+), 3.55 MeV (4^+), 3.63 MeV (0^+), 3.92 MeV (2^+), 4.45 MeV (1^-), 5.09 MeV (3^-), 5.25 MeV (2^+), 5.52 MeV (2^-), and 7.12 MeV (4^+), as indicated in the level scheme of Fig. 2. Also shown in this figure is the theoretical energy spectrum corresponding to the wave functions by Zuker used in the microscopic model calculations. Due to the 80 keV energy resolution, the 0^+ level at 5.33 MeV and the 3^+ level at 5.37 MeV could not be resolved and they have not been included in this work.

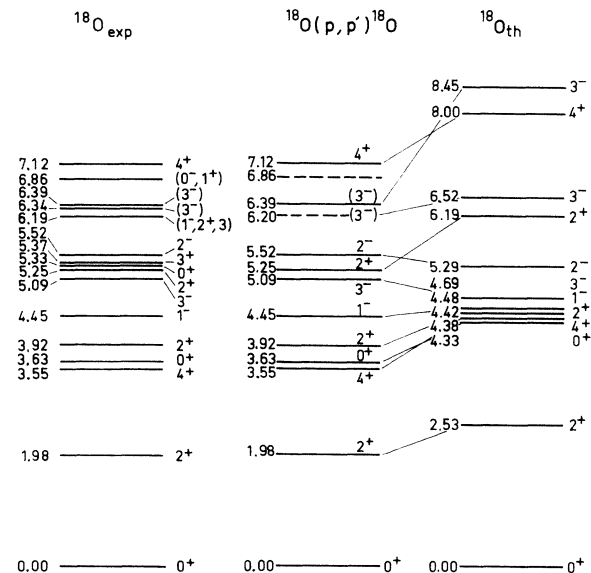


FIG. 2. Spectrum of the ^{18}O levels (left) (Refs. 40 and 41) together with the levels observed in the present experiment (middle) and correspondence with the theoretical spectrum given by Zuker's wave functions (right).

TABLE I. Optical model parameters at 24.5 MeV proton energy.

	V (MeV)	r (fm)	a (fm)	W_i (MeV)	r_i (fm)	a_i (fm)	V_s (MeV)	r_s (fm)	a_s (fm)
Elastic scattering	50.1	1.1	0.74	5.60	1.3	0.66	4.25	0.9	0.52
Inelastic scattering									
ROT ($0^+, 2^+, 4^+$)	48.92	1.1	0.70	5.05	1.52	0.58	4.30	0.9	0.44
VIB ($0^+, 3^-$)	49.49	1.1	0.70	5.07	1.41	0.60	4.30	0.9	0.44

Errors shown on the data points refer to statistical errors only. When all sources of error are taken into account, the absolute values of the elastic cross sections are estimated to be correct within 6%.

III. ANALYSIS

A. General

The cross sections and analyzing powers for all levels considered in this experiment were calculated in the distorted wave Born approximation (DWBA). Calculations in the coupled-channel approximation were performed for the 0^+ (g.s.), 2^+ (1.98), and 4^+ (7.11) within a rotational model, and for the 0^+ (g.s.) and the 3^- (5.09) in the vibrational model.

The optical model parameters have been checked for the energy dependence at 22.5 and 24.5 MeV, as discussed in Ref. 21. All sets used in the calculations reported here are listed for 24.5 MeV energy in Table I.

B. Collective model analysis

The interest in a collective model analysis is twofold:

(1) The differential cross sections and analyzing powers obtained in this experiment are, to the best of our knowledge, the only ones existing so far for proton scattering for most levels [with the exception of the 0^+ (g.s.) and 2^+ (at 1.98 MeV)(Ref. 20)].

(2) The analysis allows a qualitative test of the sizeable admixtures of collective states predicted for some levels.

The analysis was carried out with the Sherif code,²⁶ which includes the full Thomas term for the spin-orbit potential (SO). The form factor used is the deformation parameter β , times the radial derivative of the optical potential. The same procedure was used for $l=0$ and $l=1$ transitions although the collective model in these cases can only be considered as a convenient parametrization of the data. All calculations have been made with the entire optical potential deformed, since the predictions for the analyzing power are generally im-

proved by the inclusion of deformed imaginary and SO terms. It should be remarked that in this model the deformed SO term has only a very small effect on the cross section²⁷ so that its inclusion is not really necessary if only cross-section data are available. The code allows the use of a SO term with a deformation different from that of the central and imaginary potentials, but this option has been employed only in one case. The β_L parameters used in the DWBA calculations are given in Table II, together with those of coupled-channels calculations and those derived from the available electron-scattering data.²⁸

C. Microscopic calculations with the DWBA

Calculations have been made in the framework of the antisymmetrized microscopic DWBA, using the program DWBA70 of Schaeffer and Raynal.^{29,30} This program allows a complete treatment of central, spin-orbit, and tensor terms of the $N-N$ interaction, with radial form factors of the Yukawa type. Following Kuo and Brown³¹ we have used as an effective interaction the reaction matrix G derived from the Hamada-Johnston potential.²² The hard core is handled with the separation method of Scott and Moszkowski,³² with cutoff radii of 1.07 fm for the central and tensor terms. The effect of the second order term of the triplet-even tensor force is included. The $N-N$ interaction is approximated by the sum of three different Yukawa potentials, whose ranges and depths are optimized by fitting the Fourier transforms of the different terms of the potential, i.e., the potential as a func-

TABLE II. The deformation parameters B_L .

Energy (MeV)	J^π	DWBA	Coupled channels	(e, e')
1.98	2^+	0.43	0.37 ± 0.03	0.35 ± 0.04
3.55	4^+	0.32		
3.92	2^+	0.28		
5.09	3^-	0.65	0.56 ± 0.06	0.56 ± 0.03
5.25	2^+	0.20		0.26 ± 0.02
7.11	4^+	0.23	0.18 ± 0.04	
3.63	0^+	0.13		

TABLE III. Parameters of the three Yukawa potentials used for the different terms of the N - N interaction.

Range (fm)	Depth (MeV)	Triplet even	Singlet even	LS even	LS odd	Tensor even	Tensor odd
0.3		4426.5	3185.8	-180.66	-3799.5	2370.2	-849.76
0.479		-1580.4	-1078.3	95.657	102.86	-658.7	212.25
1.343		-12.84	-14.59	0.0666	0.346	-0.686	0.230

tion of the transferred momentum. It turns out that just one Yukawa potential is adequate to reproduce the Fourier transforms in the region around zero fm^{-1} transferred momentum, which is the relevant region when direct terms only are considered. However, when exchange terms are taken into account, as in our calculations, the transferred momenta are rather around $3\text{--}4 \text{ fm}^{-1}$.

We could obtain a reasonable fit over this whole range only when three Yukawa potentials were used.

For the spin-orbit term, the Scott-Moszkowski justification for the use of a cutoff radius does not hold. However, the Fourier transform of the Hamada-Johnston spin-orbit potential with a cutoff radius of 0.7 fm is similar to that of the corre-

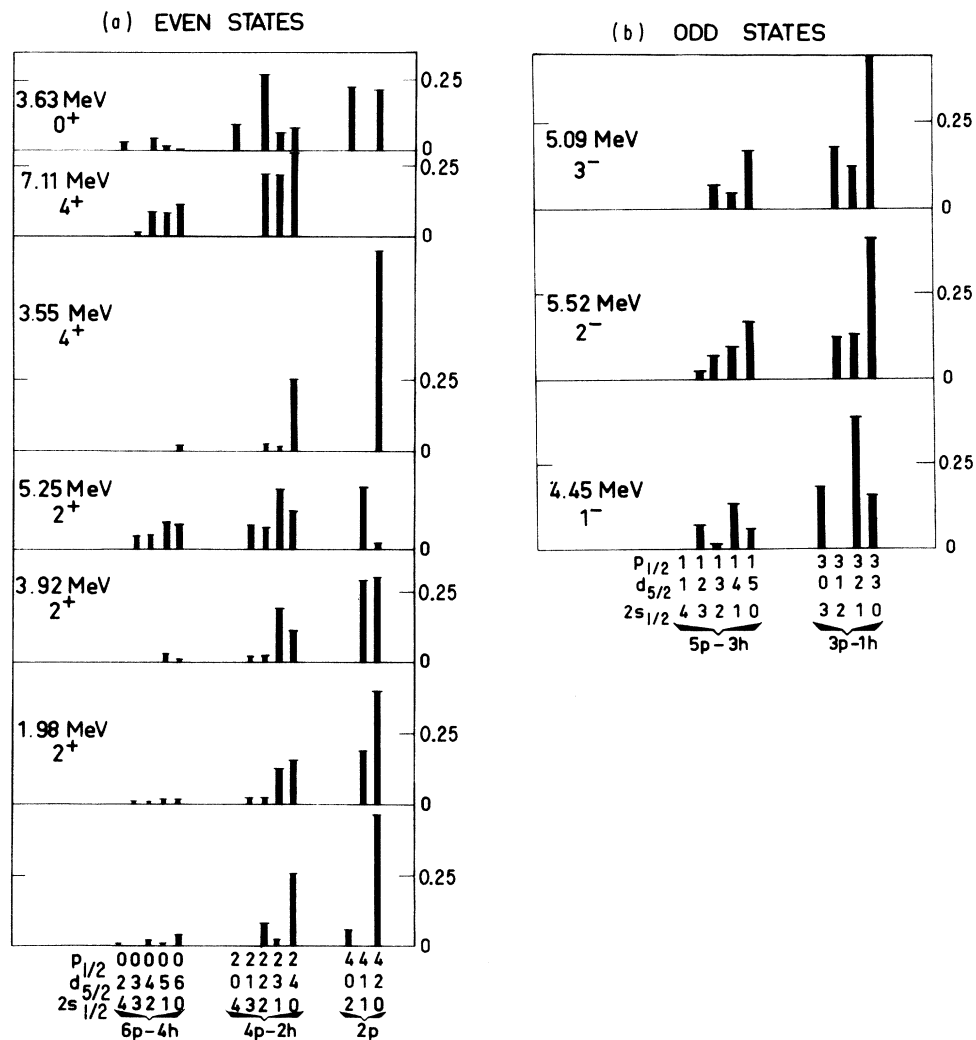


FIG. 3 (a), (b). Population, for the different levels, of the orbitals shown at the bottom according to Zuker's wave functions. The ordinate is proportional to the squares of the wave function components.

sponding terms of the Bressel potential,³³ which has a soft, square-well core. Therefore a 0.7 fm cutoff was used for the spin-orbit term. The small odd central terms, which cannot be derived through the separation method, were neglected. However, a DWBA calculation using a rough estimate of these terms showed no appreciable effects on either cross sections or analyzing powers. The parameters of the N - N interaction used are given in Table III.

Since the strength of the SO interaction is poorly known, we have systematically made calculations with both the nominal value, as derived, and a strength increased by a factor 4, in order to ascertain the effect of the term on the various transitions.

Following a suggestion of Satchler²³ efforts are underway to introduce an imaginary term in the effective N - N interaction. These studies are however only in their beginning. Some of our calculations use an imaginary form factor, proportional to the macroscopic deformation parameter, β , as employed by Terrien.³⁴

D. Wave functions

The wave functions (WF) used in almost all calculations were those of Zuker.²⁴ They involve six particles, 2 protons and 4 neutrons, in the orbitals $1p_{1/2}$; $1d_{5/2}$; $2s_{1/2}$, which define the configuration space. If the closed $1p$ shell is taken as a core, the WF of even-parity states can be of the $2p$ - $0h$, $4p$ - $2h$, $6p$ - $4h$ type, while those of odd parity can be $3p$ - $1h$ or $5p$ - $3h$, the holes being in the p shell in order to satisfy parity.

The occupation probability of different orbitals for each level is represented in Fig. 3, the ordinate being equal to the sum of the squares of the WF components.

Some calculations have been carried out using Engeland's¹⁶ WF, but only for those levels for which the $2p$ - $0h$ components represent 90% of the level strength, and core excitation is neglected. These levels are the 2^+ at 1.98 and 3.92 MeV, and the 4^+ at 3.55 and 7.11 MeV. The reason is that Engeland's WF span a larger configuration space, including the $d_{3/2}$ orbital, which is important in some levels. Similar results are obtained with the $2p$ - $0h$ WF of Kuo and Brown.³¹

The WF enter the calculations through the matrix elements $Z_{j,j'}^J$ of the particle-hole excitation operator.

The transition density is defined by:

$$\rho(r, r') = \sum_{\text{configurations}} Z_{j,j'}^J G_{j,j'}^J \Phi_j(r) \Phi_{j'}(r'),$$

where $\Phi_j(r)$ are the radial WF of bound particles,

which in our case were taken as the harmonic oscillator WF, and the $G_{j,j'}^J$ is a geometrical factor defined in Ref. 30. The transition density contains the spectroscopic information concerning the transition and its local part is by definition $\rho(r, r) \equiv \rho(r)$. The contributions of the different WF add coherently near the nuclear surface in the case of a collective transition, giving rise to a local transition density peaked around the nuclear radius. By integration with the relevant multipole of the N - N interaction one gets the form factor, which will retain its surface peaked behavior with a central force, but may lose it with an excess of noncentral spin-orbit interaction.

An *a priori* check of the validity of the WF can be made by considering the ratio $\lambda_p = [B(EJ)_{\text{exp}} / B(EJ)_{\text{th}}]^{1/2}$, which provides the number by which one should multiply the Z_{proton} to get the experimental transition rates.³⁵ If we denote by Λ the ratio of experimental to theoretical (p, p') cross sections, the comparison between Λ and λ_p gives an idea of the correctness of the relative strengths of proton and neutron excitation, if one supposes that the reaction model is sufficiently accurate. As far as the nuclear structure only is concerned, an estimate of the relative proton and neutron strengths can come from the ratio $F = (\sum Z_p^2 / \sum Z_n^2)^{1/2}$. Clearly, from the point of view of the reaction dynamics, one should compare the square of the sum of the transition amplitudes. However, some qualitative considerations can be made just on the relative values of Λ , λ_p , and F . For example, if $\Lambda \gg \lambda_p$ one could say that F is too large, namely that the WF does not contain enough neutron excitation and vice versa. A summary of

TABLE IV. Parameters characterizing the relative strength of proton and neutron excitation $\lambda_p = [B(EL)_{\text{exp}} / B(EL)_{\text{th}}]^{1/2}$;

$$\Lambda = \left[\frac{d\sigma}{d\Omega}(\text{exp}) / \frac{d\sigma}{d\Omega}(\text{th}) \right]^{1/2} \text{ and } F = \left[\frac{\sum Z_p^2}{\sum Z_n^2} \right]^{1/2}.$$

Theoretical values were calculated from Zuker wave functions (Ref. 24).

Level	Energy	$B(EL)^a$ ($e^2 \text{fm}^{2L}$)	λ_p	Λ	F
2^+	1.98	45	4	1.73	0.184
2^+	3.92	8.3	1.87	3.16	0.2
2^+	5.25	24	1.41	5	1.78
3^-	5.09	1120	0.87	3.9	2.12
0^+	3.63			2	0.87
4^+	3.55			1.4	0
4^+	7.11			0.703	0
1^-	4.45			6.3	35
2^-	5.52			3.16	4.12

^a Reference 28.

TABLE V. Summary of the available wave functions for even-parity states.

Configuration	(<i>d,p</i>) reaction Ref. 37	Kolltveit (<i>t,p</i>) Ref. 18	Federman- Talmi Ref. 15	Federman- Talmi Ref. 36	Brown Ref. 14	Engeland Ref. 16	Benson Irvine Ref. 17	Zuker Ref. 24
0 ⁺	(<i>d</i> _{5/2}) ²	81	56	71	77	44	72	46
g.s.	(<i>s</i> _{1/2}) ²	15	18.1	14	9.6	19	15	5.5
	Core exc.	4	26	15	12.2	37	9	48.5
2 ⁺	(<i>d</i> _{5/2}) ²	56	48	89	86.6	17	41	40
1.98	<i>d</i> _{5/2} <i>s</i> _{1/2}	23	26	9	6.8	33	40	19
	Core exc.	21	26	2	6.8	50	16	41
2 ⁺	(<i>d</i> _{5/2}) ²		44	2	11.6		55	50
3.92	<i>d</i> _{5/2} <i>s</i> _{1/2}		55	61	77		37	40
	Core exc.		1	37	11.6		7.2	10
2 ⁺	(<i>d</i> _{5/2}) ²	<8	10	8	2	4	1	0
5.25	<i>d</i> _{5/2} <i>s</i> _{1/2}	32	20	31	16	50	19	30
	Core exc.	>60	70	61	81	46	76	70
4 ⁺	(<i>d</i> _{5/2}) ²	80					90	94
3.55	<i>d</i> _{5/2} <i>d</i> _{3/2}						6	4
	Core exc.	20					4	2
4 ⁺	(<i>d</i> _{5/2}) ²					3.8		0
7.11	<i>d</i> _{5/2} <i>d</i> _{3/2}						85	32
	Core exc.						11	68
0 ⁺	(<i>d</i> _{5/2}) ²	<18	42	25	22	56	23	19
3.63	(<i>s</i> _{1/2}) ²		41	66	37.2	17	64	0
	Core exc.		17	9	41	27	13	81

these parameters for the transitions studied is given in Table IV.

One can therefore attempt to renormalize the proton and neutron Z 's, introducing also for the latter a multiplicative factor λ_n . In principle the way to do it is to calculate λ_p if the experimental $B(EJ)$ is known, and then vary λ_n so as to get a correct normalization of the absolute cross section. Our calculations have been carried out following this method only for the 2⁺ and the 3⁻ states, where the $B(EJ)$ are well known. In the other cases we set $\lambda_p = \lambda_n = \Lambda$ in order to normalize to the measured cross sections. The normalization of Z_p and of Z_n with $\lambda_p \neq \lambda_n$ produces a distortion of the original WF, but in our case this effect was negligible since the transitions are predominantly either neutron or proton excitations, as shown by the values of F . The only exception is for the 2⁺ level at 5.25 MeV ($F = 1.78$).

The imaginary form factor (FF) used for some calculations is the derivative of the imaginary part of the optical model potential, times the macroscopic deformation parameter β taken equal or very close to the parameters listed in Table II. Calculations were made only with properly normalized Z 's as explained above so as to assure that the relative contributions of the imaginary procedure and real parts are more or less cor-

rect. In other words with this procedure the ratio of the real to the imaginary FF is approximately equal to that of the macroscopic model. It should be stressed that the imaginary FF does not have any quantitative justification but its need and success in the macroscopic model. To us its use in microscopic calculations makes sense only when the real FF of the transition has a collectivelike behavior, i.e., it is peaked at the nuclear surface.

In the following, standard calculations, i.e., with the N - N interaction as derived and including the exchange term, are labeled "a" for Zuker's WF and "i" for Engeland's. Curves b refer to a direct calculation without exchange term and curves c to the increase of the SO term by a factor 4 in a standard calculation. Calculations with the inclusion of an imaginary FF are labeled "d" and "j," respectively, for Zuker's and Engeland's WF.

IV. EVEN-PARITY STATES

A summary of the available information on the WF of these states is given in Table V. We have written down the percentage of the 2p-0h components taken into account by the listed authors, the remaining part of the WF being ascribed to core excitation, or, in a shell model language, to 4p-2h and 6p-4h states.

A. 2^+ states at 1.98, 3.92, and 5.25 MeV

The cross sections and analyzing powers ($d\sigma/d\Omega$ and A_p) are presented in Fig. 4 together with macroscopic model calculations. Dashed curves refer to the coupled-channel calculations of Ref. 21, carried out with the parameters of Table I, while solid lines present the DWBA results.

The angular distributions show some similarity, especially between the 1.98 and 3.92 MeV levels, but the analyzing powers of these same levels are quite different. In fact a greater similarity exists at least up to 110° c.m. between the 1.98 and 5.25 MeV levels, both in $d\sigma/d\Omega$ and A_p .

1.98 MeV level

The coupled-channel calculations improve the fits to the cross sections beyond 100° with respect to the simple DWBA. The value of $\beta_2 = 0.37$ is significantly below the 0.43 of the DWBA and in much better agreement with the value derived from (e, e') data. This level had been observed previously in (p, p') and (α, α') experiments^{20, 38} and values of $\beta_2 = 0.26-0.30$ were derived. Evidence for a large collective component also comes from the $^{17}\text{O}-(d, p)^{18}\text{O}$ reaction performed by Moreh and Daniels,³⁷ who quote a 21% collective admixture, and from the

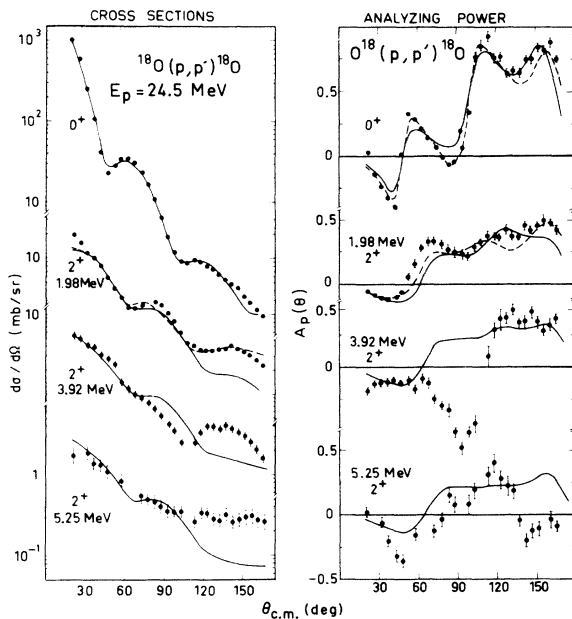


FIG. 4. Differential cross sections and analyzing powers for the g.s. and the 2^+ levels observed in this experiment. Dashed lines refer to the results of coupled-channel calculations, according to the parameters given in Tables I and II. Continuous curves are the results of the optical model fit for the g.s., according to the parameters of Table I, and of macroscopic model fits for the 2^+ , with the values of Table II.

analysis of Kolltveit, Muthukrishnan, and Trilling¹⁸ of the $^{16}\text{O}(t, p)^{18}\text{O}$ reaction, where a 25% deformed component is found. This is in fair agreement with the theoretical results listed in Table V, except for the values of Federman and Talmi^{15, 36} which are quite small and probably not consistent either with the present analysis or the above experimental evidence.

For this level the Zuker WF gives $\lambda_p = 4$, thus underestimating the observed $B(E2)$ transition rate, and therefore the proton excitation. The microscopic calculations are presented in Figs. 5 and 6. The curves of Fig. 5 imply a factor 9 normaliza-

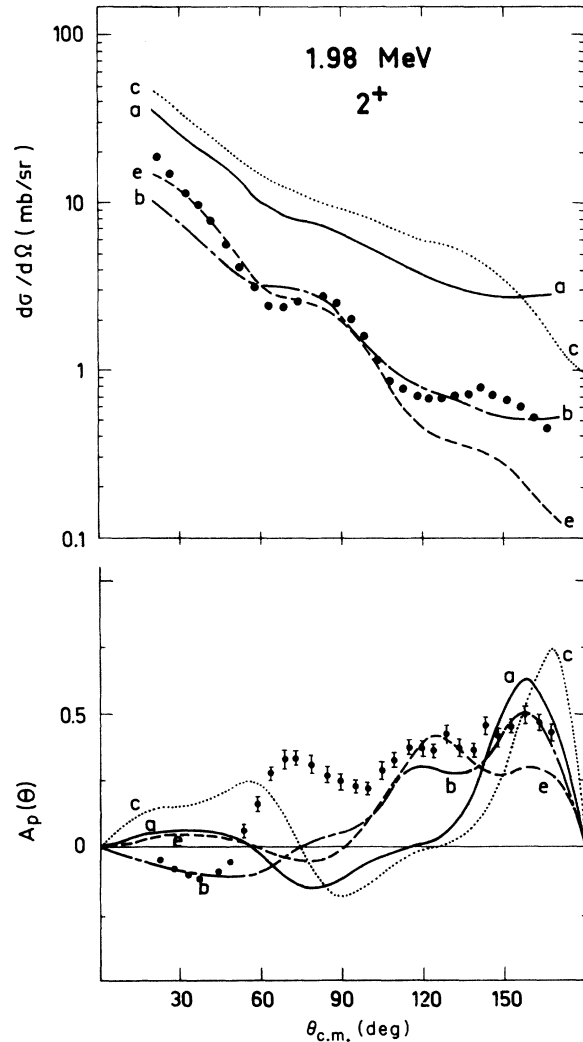


FIG. 5. Microscopic model results for the 2^+ at 1.98 MeV, using Zuker's wave functions. All curves refer to a normalization factor (see text) $\lambda_p = \lambda_n = 3$. Curves a and c refer to a standard calculation, with exchange term, the SO term being 4 times higher for c. Curves e and b are the results of a direct calculation without exchange, where for e an imaginary form factor $\beta = 0.4$ has been added.

tion of the direct calculation, labeled b, obtained by setting $\lambda_p = \lambda_n = 3$. As a result curve a, which includes the exchange, is higher than the data, and the same is true for curve c with the SO term times 4. The curves of Fig. 6 are normalized instead in a standard calculation, with $\lambda_p = \lambda_n = 1.73$ for Zuker WF (a and d) and $\lambda_p = \lambda_n = 3.16$ for Engeland's i. Calculations were also carried out with $\lambda_p = 4$, as required by the experimental $B(E2)$, and then normalizing the cross sections with $\lambda_n = 1.6$, but since the transition is predominantly due to neutron excitation, as shown by the value of $F = 0.184$, no appreciable effect is found.

As a general feature, the inclusion of the exchange term gives a somewhat structureless angular distribution of the cross sections, but the addition of the imaginary FF, curve d, restores a correct shape. The real FF of the WF has a collectivelike shape, peaked at the surface, but of in-

sufficient amplitude. This is the physical reason why the direct calculation with an imaginary FF, curve e, is very close to the macroscopic model results (Fig. 4).

The only satisfactory results obtained for the A_p are from the direct calculation, curve b. A larger SO term gives even worse results because, as mentioned before, the FF loses in this case its collectivelike behavior.

3.92 MeV level

The 3.92 MeV transition is not well fitted by the macroscopic DWBA, Fig. 4, except at very forward angles. The value $\beta_2 = 0.28$ given in Table II has therefore little physical significance. From (α, α') data β_2 values of 0.18 and 0.21 have been derived,³⁸ but the fit was in our view not satisfactory either, especially at forward angles. From

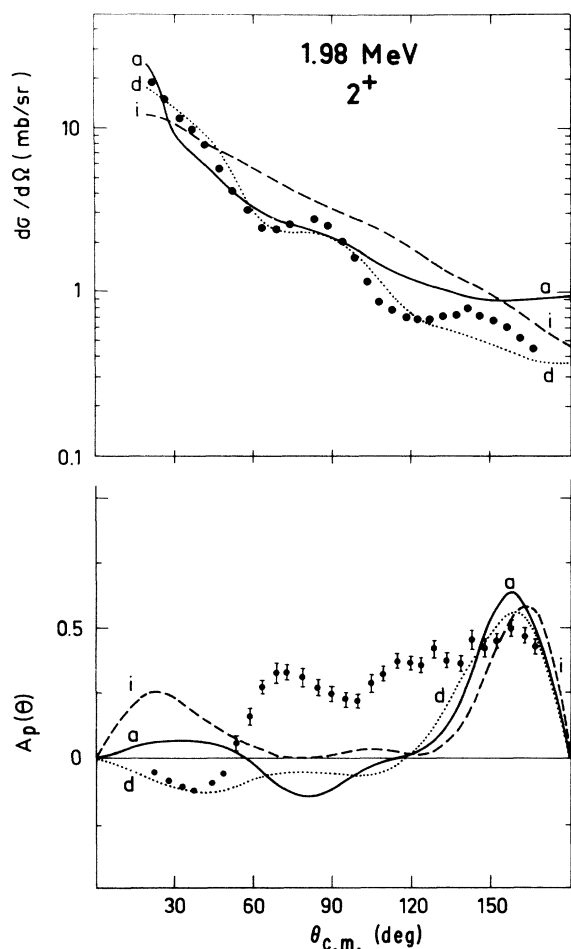


FIG. 6. Microscopic model results for the 2^+ at 1.98 MeV. Curves a and d are normalized with $\lambda_p = \lambda_n = 1.73$, d referring to an imaginary FF of $\beta = 0.4$. Curve i uses Engeland's wave functions, with $\lambda_p = \lambda_n = 3.16$.

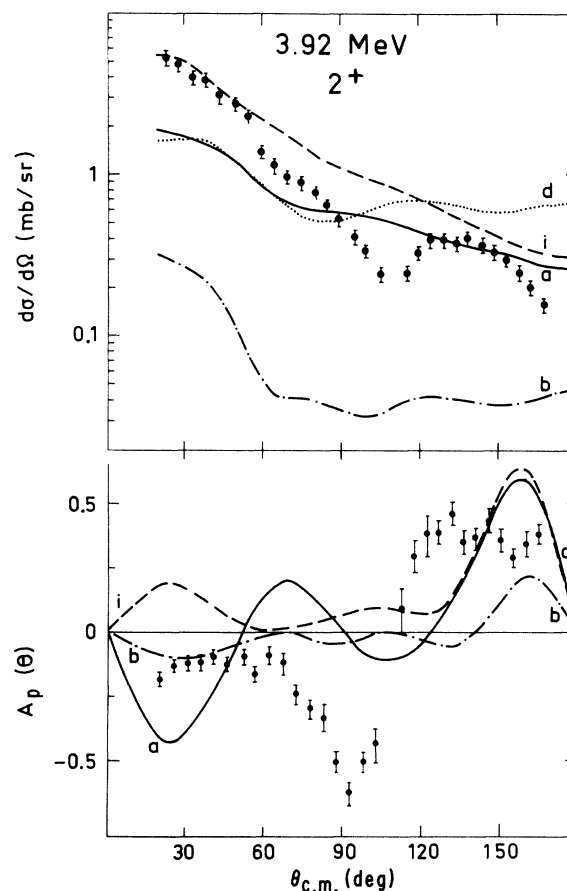


FIG. 7. Microscopic model results for the 2^+ at 3.92 MeV. Curves a, b, and d use Zuker's wave functions, with $\lambda_p = \lambda_n = 3.16$. Curve d refers to an imaginary form factor with $\beta = 0.3$, and b does not include the exchange term. Curve i uses Engeland's wave functions, with $\lambda_p = \lambda_n = 1.41$, in a standard calculation.

the $^{17}\text{O}(d, p)^{16}\text{O}$ reaction a marked $L=0$ dependence was found for this level,³⁹ which would indicate a sizeable ($d_{5/2}s_{1/2}$) component in the WF. From the analysis of (t, p) reactions Kolltveit *et al.*¹⁸ obtain only a 2.5% deformed component against 55% for ($d_{5/2}s_{1/2}$) and 42% for ($d_{5/2}$)². Theoretical predictions are scattered, as shown in Table V, but with generally low estimates of core excitation. Since this level should have little collective nature the fact that our β_2 value is in agreement with the $\beta_2 = 0.16$ deduced from (e, e') data does not have much meaning. This conclusion is also substantiated by the quoted branching ratios to the 1.98 MeV level and the ground state (g.s.), respectively, 85 and 15%.⁴⁰

The microscopic calculations are presented in Fig. 7. The values of $\lambda_p = 1.87$ and $\Lambda = 3.16$ indicate that the transition lacks neutron excitation, although this is already dominant in the WF ($F = 0.2$). The fits for either Zuker and Engeland WF are not satisfactory.

The form factor is peaked well into the interior of the nuclear surface, with a zero at the nuclear

radius, so that the use of an imaginary FF, curve d, is not justified. Since Zuker WF apparently contains too much core excitation with respect to the above experimental evidence, we have also tested Kuo and Brown³¹ 2p-0h WF but the results are even worse. Perhaps the "true" WF is much more complex than the ones now available.

5.25 MeV level

The 5.25 MeV transition is well fitted by the macroscopic model both in $d\sigma/d\Omega$ and A_p , up to 120° , Fig. 2. The $\beta_2 = 0.20$ agrees with the 0.26 derived from (e, e') data.²⁸ The worse fit at larger angles is not surprising, since a similar situation exists for the 1.98 MeV level, which is improved only by coupled-channel calculations. Independent evidence for a strong deformed component comes from (d, p) reactions^{37, 39} and from the analysis of (t, p) data,¹⁸ which yield, respectively, 60 and 70% for core excitation admixture. This state was found to be strongly excited in the $^{14}\text{C}(^7\text{Li}, t)^{18}\text{O}$ reaction,⁴¹ indicating a low single particle compo-

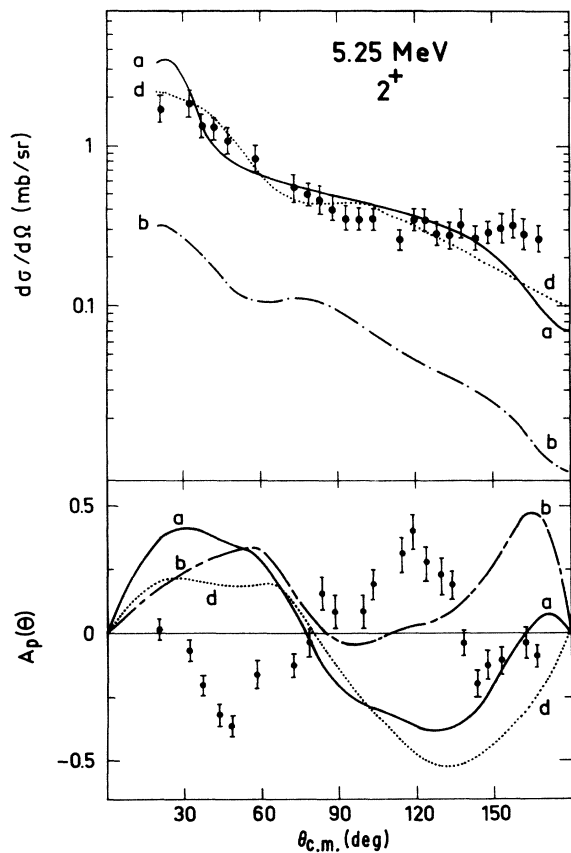


FIG. 8. Microscopic model results for the 2^+ at 5.25 MeV. All curves use Zuker's wave functions, with $\lambda_p = \lambda_n = 5$. Curve d refers to an imaginary form factor with $\beta = 0.2$.

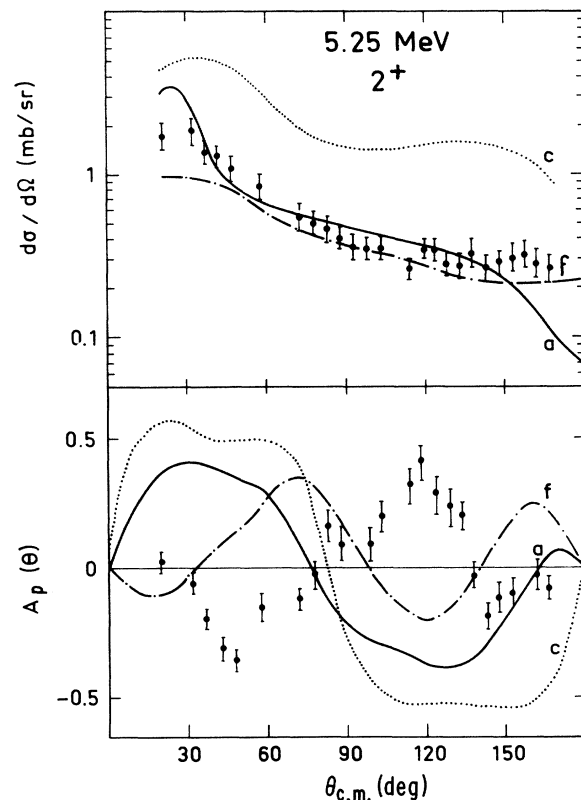


FIG. 9. Other microscopic results for the 2^+ at 5.25 MeV, with Zuker's wave functions. The normalization for a and c is as in Fig. 8, in c the SO term is 4 times the standard value. Curve f is another standard calculation but with a normalization given by $\lambda_p = 1.41$, $\lambda_n = 9.9$ (see text).

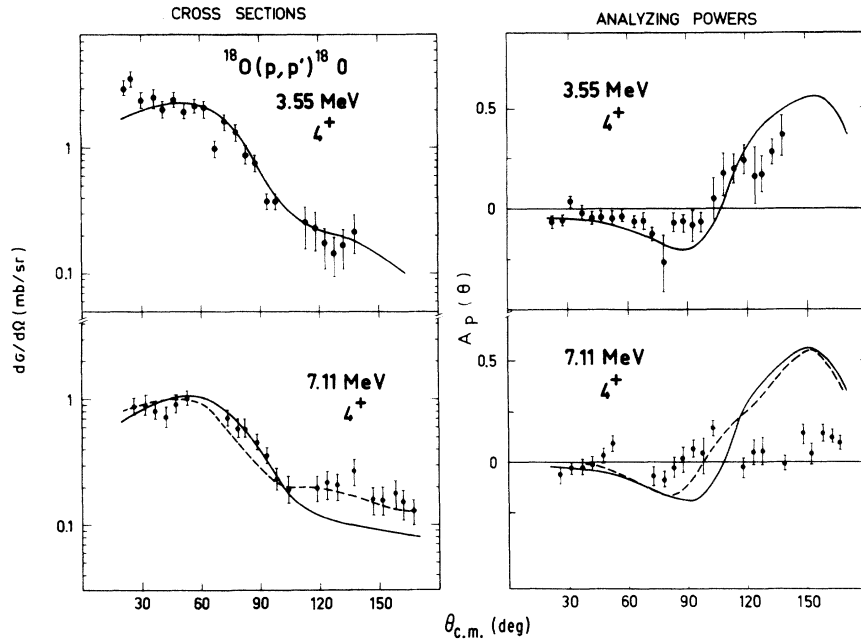


FIG. 10. Experimental data and macroscopic model calculations for the 4^+ at 3.55 and 7.11 MeV. Continuous curves are obtained with the parameters of Table II. Dashed lines refer, for the 7.11 MeV level, to coupled-channel calculations (see Table II and text).

ment and a large α particle component in the wave function, thus pointing toward sizeable $4p$ - $2h$ components. It has been suggested that this level belongs to a rotational band based on the 0^+ state at 3.63 MeV, having as a further member the 4^+ state at 10.29 MeV.⁴² No evidence for this could be gathered from our data.

The microscopic calculations are presented in Figs. 8 and 9. The value of $\lambda_p = 1.41$ indicates that the Zuker WF, which contains mainly a proton excitation, reproduces fairly well the experimental $B(E2)$. Since, however, the normalization factor Λ is about 5, there is probably a lack of neutron excitation. According to these considerations, the curves of Fig. 8 refer to $\lambda_p = \lambda_n = \Lambda = 5$, and the same is true for curves a and c of Fig. 9. Curve f instead is calculated with $\lambda_p = 1.41$ and normalizing then the cross sections with $\lambda_n = 9.9$.

An acceptable fit to the $d\sigma/d\Omega$ is obtained by either a and f, differing only in the ratio of proton to neutron normalization, but the results are disappointing for the A_p . The latter is completely out of phase with the data, suggesting that the fit to the cross section could be fortuitous. In fact the real FF for this transition is peaked inside the nucleus, in sharp contrast with that for the 1.98 MeV level, even though the two (p, p') angular distributions are similar, as noted earlier. On the other hand, since the $2p$ - $0h$ components of the WF agree with the data from (d, p) and (t, p) reactions, a

likely explanation is that the description of core excitation is not correct.

B. 4^+ levels at 3.55 and 7.11 MeV

The data for these two levels are presented in Fig. 10, together with macroscopic DWBA calculations. The angular distributions are similar, although distinguishable, the 3.55 MeV level being about 2.5 times more strongly excited than the 7.11 MeV level. The A_p are also similar up to about 110° . The DWBA fits well the 3.55 MeV transition with $\beta_4 = 0.32$, and less satisfactorily the 7.11 MeV level. The latter is much improved by coupled-channel calculations, shown as a dashed line, a fact presented in Ref. 21 as evidence for a rotational band based on the g.s.

The 3.55 MeV level was observed in the $^{17}\text{O}(d, p)$ reaction³⁷ as proceeding through an $L=2$ angular momentum transfer, and in the $^{16}\text{O}(t, p)$ reaction⁴³ as an $L=4$ transfer. From the (d, p) reaction data, this level should have an 80% $(d_{5/2})^2$ component, and 20% deformed. Much lesser values of the latter are given by some authors, see Table V. The present results support more the estimates from the (d, p) reaction than the low theoretical values.

The results for the 7.11 MeV level are consistent with a collective nature and a coupling to the g.s. and the 2^+ level at 1.98 MeV. This level is strongly populated by the $^{14}\text{C}(^7\text{Li}, t)$ reaction⁴¹ and

also strongly excited by the $^{14}\text{C}(\alpha, \gamma)$ reaction,^{44, 45} suggesting that it contains a high parentage of a configuration involving a ^{14}C core plus an α particle. This is equivalent to core excitation of ^{18}O . From $^{17}\text{O}(d, p)$ data this level should contain about 20% ($d_{5/2}d_{3/2}$) configuration.⁴⁶ The large deformed state admixture predicted theoretically, Table V, seems consistent with our macroscopic model results.

As for the microscopic calculations, the only transition in Zuker's configuration space which produces a 4^+ is within the $d_{5/2}$ orbital. The intensity of such a transition is proportional to the overlap of the WF of the g.s. and the two 4^+ levels, visualized in Fig. 3. The overlap is 7 times larger for the first 4^+ than for the second, while the ratio of (p, p') cross sections is 2.5, as noted above. This discrepancy points out that at least one of the WF cannot be correct. In fact the above arguments

for the 7.11 MeV level indicate that the absence of the $d_{3/2}$ orbital, present in Engeland's configuration space, limits the completeness of the WF. Calculations with Zuker WF, not presented here, give results similar to those with Engeland WF for the 3.55 MeV level, but worse for the 7.11 MeV level.

The results are shown in Figs. 11 and 12 for the 3.55 and 7.11 MeV levels. The best fits are obtained with the addition of an imaginary FF of $\beta=0.32$ and $\beta=0.19$, respectively, normalizing with values of $\lambda_n=\lambda_p=\Lambda$, equal to 1.41 and 0.703, respectively. The agreement found by using the imaginary FF is consistent with the macroscopic results, and the fact that the real FF are peaked at the nuclear surface. A qualitative agreement exists also for the A_p , especially for the 3.55 MeV level.

C. 0^+ level at 3.63 MeV

No good fits are obtained in the macroscopic DWBA for the 0^+ level, as shown in Fig. 13 for a β value of 0.13. The $d\sigma/d\Omega$ is only tentatively reproduced while the A_p shows a 10° phase shift with respect to the data for angles larger than 40° .

This state is excited as strongly as the 2^+ at 5.25

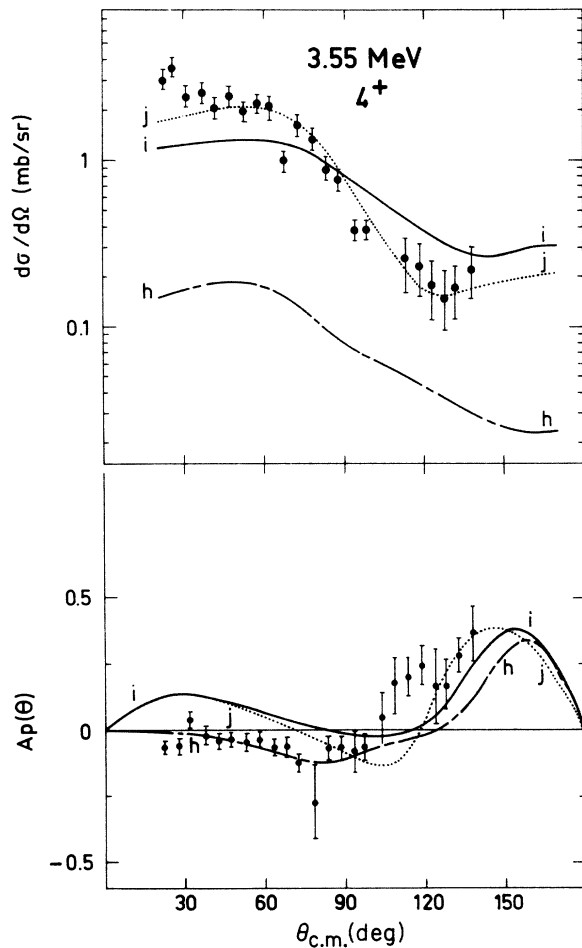


FIG. 11. Microscopic model results for the 3.55 MeV level and Engeland's wave functions with a normalization given by $\lambda_p=\lambda_n=1.41$. Curve i is a standard calculation, j refers to an imaginary form factor of $\beta=0.32$, h is a direct calculation without exchange term.

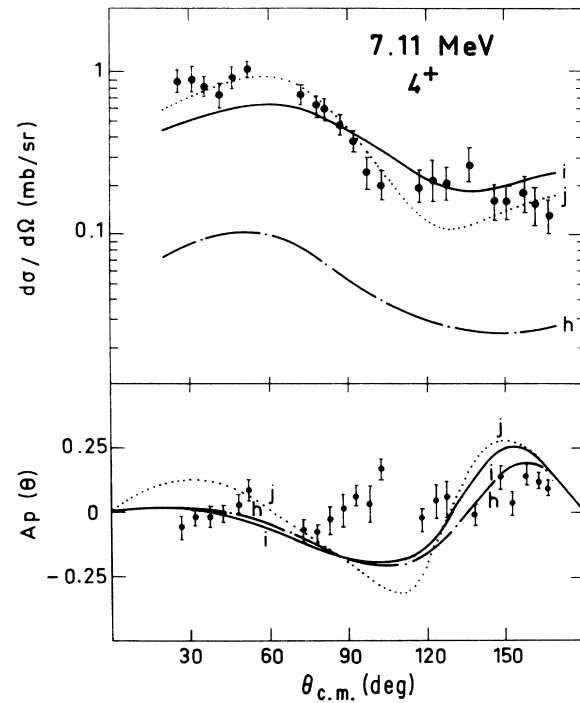


FIG. 12. Microscopic model results for the 7.11 MeV level and Engeland's wave functions with a normalization given by $\lambda_p=\lambda_n=0.703$. Curve i is a standard calculation, j refers to an imaginary form factor of $\beta=0.19$, h is a direct calculation.

MeV, to which it has been suggested to be coupled through a second rotational band.⁴² Our results are, however, disappointing in this respect. This level is weakly excited in (d, p) reactions,^{37, 47} yielding less than 18% component of $(d_{5/2})^2$. The analysis of (t, p) data led however to an estimate of 42% $(d_{5/2})^2$, 41% $(s_{1/2})^2$, and 16% core excitation.¹⁸ Our calculations show that if a collective component is present it is indeed very small, or else the mechanism for exciting this level is not a simple one-step process.

As for the microscopic model results, shown in Fig. 14, the fit of curve a is reasonable up to 120° , while the A_p behavior is not reproduced. The introduction of an imaginary FF improves the fit to the cross section, but its use is scarcely meaningful since the real FF is peaked at the interior of the nucleus. Calculations with Kuo-Brown WF³¹

show an equally bad fit, but the absolute value of the cross section is about right, instead of the factor 4 normalization needed for Zuker WF.

V. ODD-PARITY STATES

A. 1^- state at 4.45 MeV

No acceptable fits were obtained for this transition with a macroscopic model. This level had been proposed earlier⁴⁸ as a member of a negative-parity band, i.e., 1^- , 3^- , 5^- which prompted us to try a macroscopic fitting. Our data show that it is about one order of magnitude less excited than the 3^- , besides the fact that no macroscopic model fit is achieved. Thus our experiment does not support the above hypothesis.

Since this level is weakly excited in (d, p) and

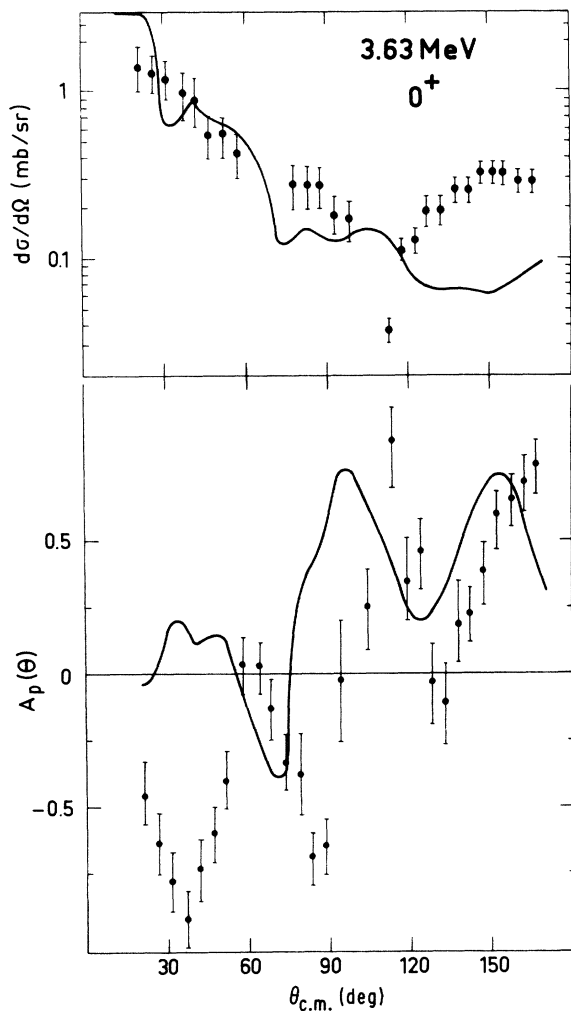


FIG. 13. Experimental data and macroscopic model results for the 0^+ level at 3.63 MeV. The calculations use a β value of 0.13.

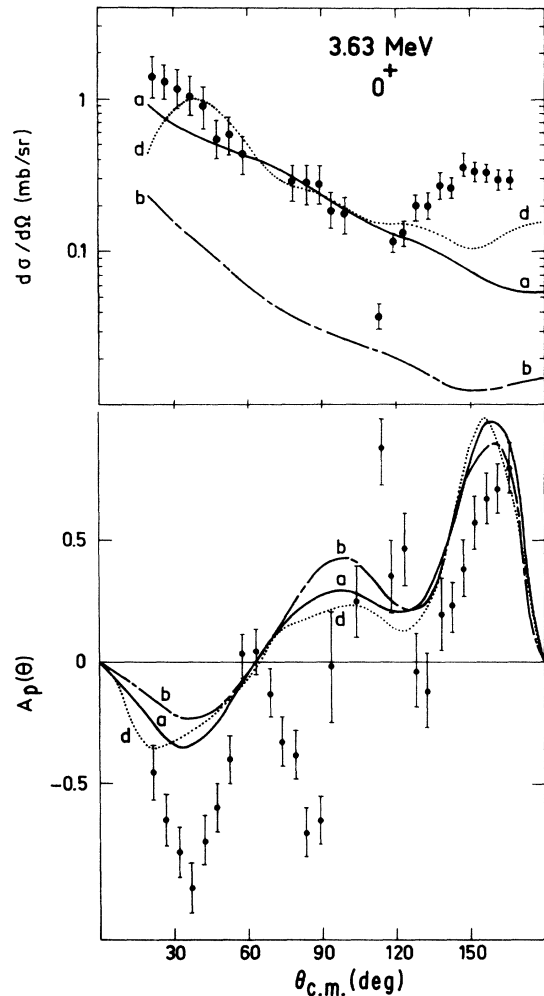


FIG. 14. Microscopic model results for the 0^+ at 3.63 MeV, using Zuker's wave functions and a normalization given by $\lambda_p = \lambda_n = 2$. Curves a and b are, respectively, standard and direct only calculations while d refers to an imaginary form factor with $\beta = 0.13$.

(t, p) reactions,^{37, 39, 43} and strongly excited by ^{19}F -($d, ^3\text{He}$)⁴⁹ and $^{19}\text{F}(t, ^4\text{He})$ reactions,⁵⁰ an important component of its configuration could arise from the lifting of a proton from the $1p$ shell into the $2s-1d$ shell. In fact, the Ellis-Engeland WF¹⁹ describes it as a $3p-1h$ state with two neutrons and one proton in the $s_{1/2}$ and one proton hole in the $p_{1/2}$ shells.

It is worth recalling that also angular distributions from (α, α') experiments could not be fitted with the one-step DWBA.³⁸ Similar situations have arisen in the past, e.g., in the case of $^{20}\text{Ne}(\alpha, \alpha')$ reported by Springer and Harvey,⁵¹ who suggested that their 1^- level could be fed through a two-step process via the excitation of a 3^- . Such a hypothesis could hold also in this case.

No acceptable fits could be obtained either in the microscopic model as shown, mostly for the pur-

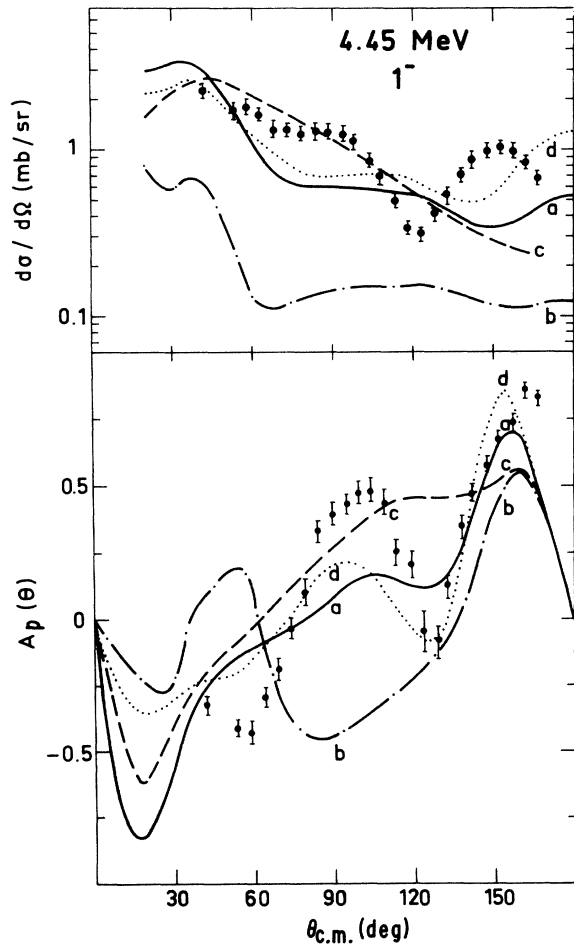


FIG. 15. Microscopic model results for the 1^- level at 4.45 MeV, using Zuker's wave functions and a normalization given by $\lambda_p = \lambda_n = 6.3$. Curve d refers to an imaginary form factor, with $\beta = 0.3$, while a, b, and c have the usual meaning of standard, direct only, and standard with 4 times higher SO term, respectively.

pose of presenting the data, in Fig. 15. The transition is described by Zuker WF as a proton hole in the $p_{1/2}$ shell, lifted into the $s_{1/2}$ shell. This is however the only significant component while in reality the nature of the level could be more complex. Again, as shown in Fig. 15, only the addition of the imaginary FF produces a structure, both for $d\sigma/d\Omega$ and A_p , in better agreement with the data. Since however the real FF is peaked at about half the nuclear radius the meaning of the imaginary FF is doubtful.

B. 3^- state at 5.09 MeV

Data and calculations for this level, whose spin and parity have been assigned only recently,⁵² are shown in Fig. 16. Coupled-channel calculations in the vibrational model, i.e., coupling the g.s. and 3^- , are drawn with dashed lines. Both DWBA and coupled-channel calculations use a SO term 1.4 times larger than the central ones, to improve A_p fits. The fits are satisfactory, the β_3 values of 0.65 in the DWBA and 0.56 in the coupled-channel

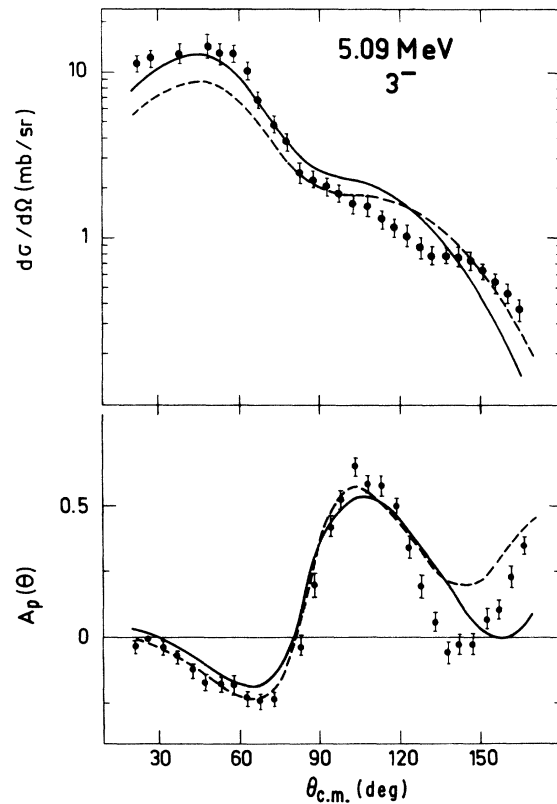


FIG. 16. Experimental data and macroscopic model results for the 3^- level at 5.09 MeV. Dashed lines refer to coupled-channel calculations with parameters given in Tables I and II. Continuous curves give the deformed DWBA results with the parameter $\beta = 0.65$, as from Table II.

case being in agreement with the one derived from (e, e') data. This analysis yields therefore evidence for the collective nature of this level, which is about as strongly excited as the 2^+ level at 1.98 MeV.

This transition had been observed, but not completely resolved, in an early (α, α') experiment,³⁸ which yielded a β_3 of 0.4 but with not very satisfactory fits at forward and backward angles. The level is weakly excited in (d, p) ⁴⁷ and (t, p) reactions,⁴³ while it comes out strongly in the ^{14}C - $(^7\text{Li}, t)$ reaction,⁴¹ suggesting that it could arise from a proton out of the ^{16}O core. According to recent calculations of Ellis and Engeland¹⁹ this should be essentially a $3p$ - $1h$ state, with two neutrons and one proton in $(d_{5/2})$ and one proton hole in $(p_{1/2})$.

The Zuker WF predicts mainly a proton excita-

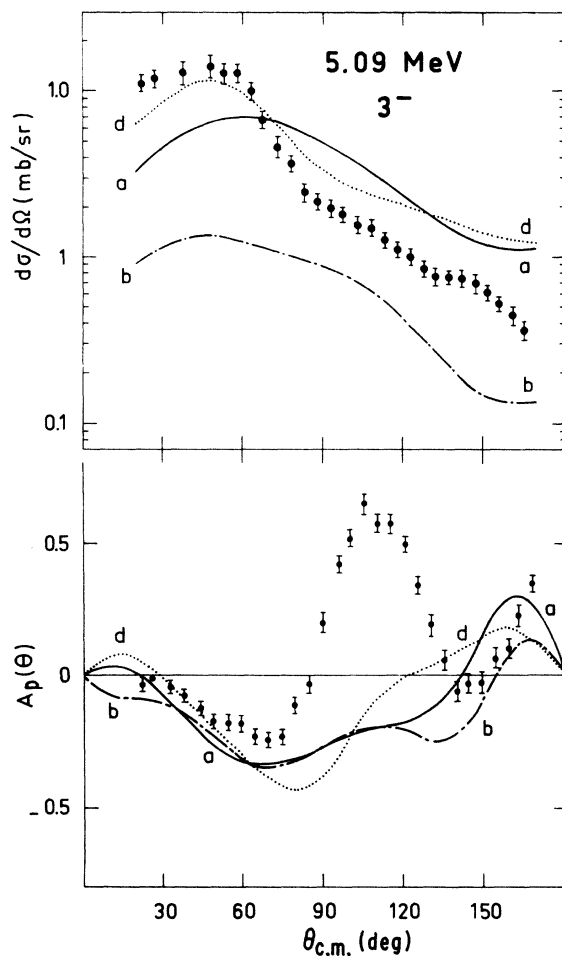


FIG. 17. Microscopic model results for the 5.09 MeV level, using Zuker's wave functions, and a normalization given by $\lambda_p = \lambda_n = 3.9$. Curves a and b have the usual meaning, curve d referring to an imaginary form factor with $\beta = 0.65$.

tion, which appears to be slightly overestimated since $B(E3)_{th} > B(E3)_{exp}$ with $\lambda_p = 0.87$. The curves of Fig. 17 correspond to a normalization of $\lambda_p = \lambda_n = 3.9$. Calculations with $\lambda_p = 0.87$, as required by the $B(E2)$ comparison, and $\lambda_n = 7.6$, showed little difference. The best fit is certainly obtained with an imaginary FF, curve d. The effect of varying the β is shown in Fig. 18, with larger β giving a better agreement with the A_p data. Since the real FF for the transition is peaked at the nuclear radius the use of an imaginary FF seems correct.

C. 2^- level at 5.52 MeV

This is the only unnatural parity level observed in this experiment. Previous experimental evidence^{39, 43} suggests that its configuration arises mainly from the lifting of a proton from the $p_{1/2}$ into the s - d shell. Accordingly Zuker WF describes the transition as due to proton excitation, with a form factor which is surprisingly peaked

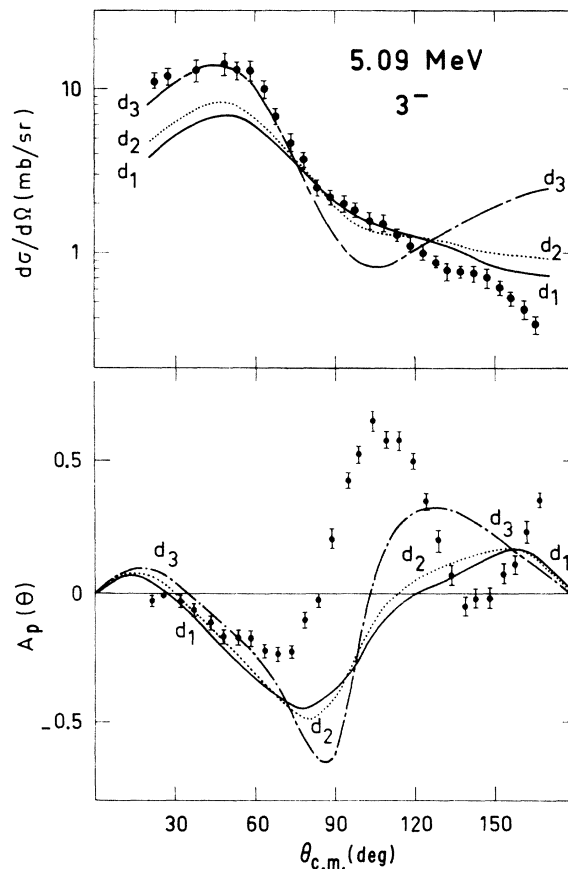


FIG. 18. Microscopic model results for the 5.09 MeV level, showing the effect of a variation of the amplitude of the imaginary form factor. All curves use Zuker's wave functions, with $\lambda_p = \lambda_n = 1.73$. The d_1 , d_2 , and d_3 lines use β values which are, respectively: 0.29, 0.40, and 0.80.

near the nuclear surface. Microscopic calculations are shown in Fig. 19. They correspond to a $\lambda_p = \lambda_n = 3.16$, because of a lack of normalization of about a factor 9. From Fig. 19 it looks like a better agreement is obtained with curve c, namely by increasing the SO term.

VI. GENERAL TRENDS

We wish to summarize here the main points which emerge from this analysis. The macroscopic model works reasonably well on a number of levels, i.e., the 2^+ at 1.98 and 5.25 MeV, the 3^- and the two 4^+ at 3.55 and 7.11 MeV. With this, we suggest that all those levels have a collective nature, although the collective model is not fully appropriate to describe their excitation. On the other hand the success of these very simple, one-parameter DWBA calculations, all the more remarkable because of the agreement with β 's derived from (e, e') , is a fact which cannot be dismissed and can hardly be regarded as fortuitous.

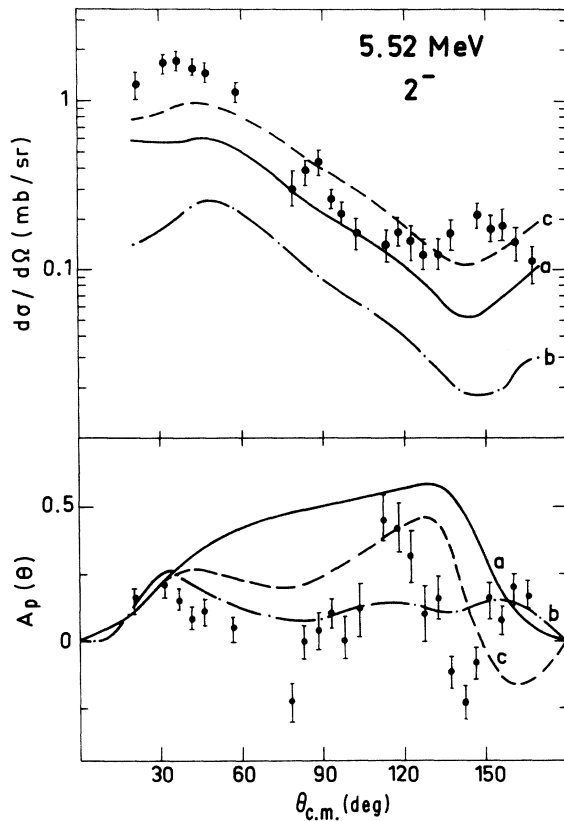


FIG. 19. Experimental data and microscopic model results for the 2^- level at 5.52 MeV. The calculations use Zuker's wave function with a normalization given by $\lambda_p = \lambda_n = 3.16$, and the usual meaning for curves a standard, b direct only, and c standard with SO term increased by a factor 4.

TABLE VI. Ratios of calculated total cross sections in the microscopic model, referred to Zuker's wave functions. Values in parentheses refer to Engeland's wave functions. See text for symbol explanation.

Level	Energy (MeV)	$\rho_1 = \frac{D+E}{D}$	$\rho_2 = \frac{D+E+I}{(D+E)}$	$\rho_3 = \frac{(D+E)4LS}{(D+E)1LS}$
2^+	1.98	3.43 (4.35)	1.15	3.2
2^+	3.92	9.47	1.086	1.3
2^+	5.25	5.6	1.16	4.5
4^+	3.55	10.7 (8.46)	1.3 (1.22)	1.28 (1.3)
4^+	7.11	10.7 (7.02)	1.3 (1.16)	1.28
0^+	3.63	5.8	1.07	2.93
1^-	4.45	4.5	1	4.7
3^-	5.09	5.4	1.22	2.2
2^-	5.52	2.65	...	1.6

Since the only physical information which enters the calculations, apart from spin, parity, and excitation energy, is the optical potential, i.e., the information on the elastic scattering, the success of the model probably reflects a basic similarity in the way these levels are excited with respect to the g.s.

In order to appreciate the difference of the various microscopic calculations, Table VI presents some useful ratios for the total (p, p') cross sections to the various levels, namely: ρ_1 , ratio of the direct plus exchange total cross section (σ_T) to the direct only; ρ_2 , ratio of the (σ_T) with an imaginary FF, to the direct plus exchange case; ρ_3 , ratio of the σ_T with a factor 4 increase in the SO term, to the σ_T with the standard SO value.

The exchange term has a large effect in increasing the cross section with ρ_1 ratios spreading from 2.65 to 10. Basically one would expect $\rho_1 = 4$ for a zero range force, because the odd-parity central terms are neglected here as in a Serber mixture. The observed variations are therefore finite range effects, which can be different for various configurations even for the same J . Evidence from other data⁵³ is that in general the ρ_1 values are about 4 for collective 2^+ and 3^- levels, when they are well described. In our case for levels with the same spin, this is not so, suggesting that the collectivity is not well described by the WF.

It is interesting to note that for those levels for which ρ_1 is the largest, the SO term effect (ρ_3) is the smallest, as in the 2^+ level at 3.92 and the two 4^+ levels. That the SO term should be smaller for these levels can be understood because the comparison of ρ_3 and F values shows that its effects are more important when the excitation is predominantly a proton excitation. The physical reason for this is that the proton-proton SO interaction is about 2.5 times larger than the proton-neutron one.

Apart from the 2^- nonnatural parity level where the tentative agreement may be fortuitous, we have no evidence from this work that the SO term should have a larger value than that derived from the free $N-N$ potential.

The available WF generally predict cross sections which are too small with normalization factors ranging from about 1 up to 40. This is a fairly common feature of microscopic calculations at the present state of the art.⁵⁴ The cause of these insufficient amplitudes may be attributed either to the limited configuration space out of which the WF are built or to the failure to include two-step mechanisms. In our case some comments can be made:

- (i) The $N-N$ interaction used is rather complete and reasonable variations of its parameters cannot account for the observed effects. There is no evidence that the strength of the spin-orbit term is very far from the true one.
- (ii) The normalization factors needed vary substantially, with no clear pattern discernible. This could be due to the levels' description or to different contributions of nondirect transitions to each particular level.
- (iii) When different WF are used, e.g., Engeland WF for the 4^+ at 7.11 MeV, there is a definite effect on the absolute value of the cross section. A similar effect is seen for the 0^+ at 3.63 MeV when Kuo-Brown WF are used. In this context the method we have chosen to renormalize the transition densities, i.e., the multiplication by λ_p and λ_n , is not sufficient. Its advantages lie in the fact that we account for the observed electromagnetic (E.M.) transition rates, when known, and that we probably estimate correctly the effect of the imaginary FF since the cross sections are properly normalized. On the other hand, it does not account correctly for the possible effects of an enlarged configuration space, as explained below.

One could *a priori* expect that by enlarging the configuration space, the "new" WF would be obtained by adding small components to the old ones. However, some calculations, particularly those of Soyeur,⁵⁵ show that one obtains very different WF, even though the agreement with the experimental energy spectrum is preserved. That the enlargement of the configuration space is important is proved by the results of the calculations on the 4^+ level at 7.11 MeV with Zuker and Engeland WF. Recent work⁵⁶ shows that a $d_{3/2}$ component in the g.s. of ^{18}O has to be taken into account if one wants to explain (p, d) and (p, t) reactions on this nucleus.

As for the physical connection between macroscopic and microscopic calculations this is not quite clear yet. Some considerations can however

be made in the case of rotational bands, and in this sense our present knowledge of ^{18}O offers a way to compare the two methods. We recall that the coupled-channel calculations have supplied evidence for a rotational band $0^+, 2^+, 4^+$.²¹ Should the WF reproduce this band, they would show evidence for intrinsic states i.e., states with the same population in the different orbitals for the various members of the band, with only the coupling scheme changing for the different J 's. Soyeur⁵⁵ has proven, for the middle of the $s-d$ shell, that this effect cannot be seen unless the configuration space is sufficiently large. In our case this similarity can only be seen between the 0^+ g.s. and the 2^+ at 1.98 MeV, but not with the 4^+ at 7.11 MeV (Fig. 3). It is therefore only with the use of a larger space that a meaningful comparison could be made. Moreover the use of harmonic oscillator WF can be unrealistic, especially for the $2s_{1/2}$ orbital.

The cases where there is definite evidence for an improvement in the use of the imaginary FF are only those for which the real FF is collective-like, i.e., the 2^+ at 1.98 MeV, the 3^- , and the two 4^+ . This would indicate a deficiency in the description, either in the reaction mechanism or the $N-N$ interaction. It is nevertheless important to stress that the imaginary FF mostly adds structure to the angular distributions, without affecting the over-all normalization significantly.

The fits to the analyzing power are generally rather difficult to achieve, indicating that this information is a fine detail of the reaction and which is less well understood at this time. A much more extensive development of the model is probably needed to attack this side of the problem.

VII. CONCLUSIONS

It appears that the microscopic model at least partially fulfills its goal of allowing a test of the nuclear WF. This is limited in some cases by reaction mechanism problems and insufficient knowledge of the $N-N$ interaction. The uncertainties of the $N-N$ interaction cannot be responsible for the large normalization factors nor for the large discrepancies in the shapes of the cross section and analyzing power angular distributions.

In view of these findings, we think that the most hopeful improvements of the model would be in two directions:

- (1) the use of four particle-two hole wave functions in deformed (Nilsson-like) orbitals (this kind of scheme seems to give interesting results in mass 18⁵⁷ as well as in mass 42⁵⁸ nuclei); this because, while it is clear that the simple two-particle description is insufficient, the present state of

the art of shell model calculations will probably not provide for some time correct WF in a much enlarged configuration space.

(2) the investigation of multistep processes including particle transfer, like a (p, d) followed by a (d, p) reaction.

Even though the analysis reported here is quite detailed, measurements at higher energies would certainly be helpful to check the correctness of our results. As a matter of fact the availability of (p, p') data at different energies for the same levels of a given nucleus should be a standard starting point for whichever reaction model is tested. These measurements are probably as important, at this state of development, as data on

the analyzing power, at least until one has reduced somewhat the major existing discrepancies between experiment and theory.

ACKNOWLEDGMENTS

We wish to thank R. Schaeffer and A. Zuker for helpful discussions and the interest shown in this work. We are deeply indebted to M. Soyeur for carrying out the calculations of the WF and the Z' 's coefficients. We are grateful to the Saclay cyclotron crew for the constant help during the experiment, and to J. Gosset, B. Mayer, and H. Kamitsubo for assisting us during the run.

*Present and permanent address: Istituto Nazionale di Fisica Nucleare, Sezione di Milano, Italy.

- ¹W. G. Love and G. R. Satchler, Nucl. Phys. A159, 1 (1970).
- ²F. Petrovich, H. McManus, V. A. Madsen, and J. Atkinson, Phys. Rev. Lett. 22, 895 (1969).
- ³H. McManus, in *The Two-Body Force in Nuclei, Proceedings of a Symposium held at Gull Lake, Michigan, 1971*, edited by S. M. Austin and G. M. Crawley (Plenum, New York, 1972).
- ⁴H. Sherif and J. S. Blair, Phys. Lett. 26B, 489 (1968); H. Sherif, Nucl. Phys. A131, 532 (1969).
- ⁵R. de Swiniarski, A. D. Bacher, F. G. Resmini, G. R. Plattner, D. L. Hendrie, and J. Raynal, Phys. Rev. Lett. 28, 1140 (1972).
- ⁶A. B. Kurepin and R. M. Lombard, Phys. Lett. 37B, 55 (1971).
- ⁷R. de Swiniarski, C. Glashauser, D. L. Hendrie, J. Sherman, A. D. Bacher, and E. A. Clatchie, Phys. Rev. Lett. 23, 317 (1969); P. Kossanyi-Demay and R. de Swiniarski, Nucl. Phys. A108, 577 (1968).
- ⁸M. P. Barbier, R. M. Lombard, J. M. Moss, and Y. Terrien, Phys. Lett. 34B, 386 (1971).
- ⁹S. M. Austin, in *The Two-Body Force in Nuclei, Proceedings of a Symposium held at Gull Lake, Michigan, 1971* (see Ref. 3).
- ¹⁰S. M. Austin, P. J. Locard, S. M. Bunker, J. M. Cameron, J. Richardson, J. W. Verba, and W. T. H. Van Oers, Phys. Rev. C 3, 1514 (1971).
- ¹¹W. G. Love, Phys. Lett. 35B, 371 (1971).
- ¹²W. G. Love, Nucl. Phys. A192, 49 (1972).
- ¹³J. Raynal, International Atomic Energy Agency Report No. SMR 8/8, 1972 (unpublished), p. 75.
- ¹⁴G. E. Brown, in *Proceedings of the International Conference on Nuclear Physics, Paris, 1964*, edited by P. Gugenberger (Centre National de la Recherche Scientifique, Paris, 1964), Vol. 1, p. 129.
- ¹⁵P. Federman and I. Talmi, Phys. Lett. 15, 165 (1965).
- ¹⁶T. Engeland, Nucl. Phys. 72, 68 (1965).
- ¹⁷H. G. Benson and J. M. Irvine, Proc. Phys. Soc. 89, 249 (1966).
- ¹⁸K. Kolltveit, R. Muthukrishnan, and R. Trilling, Phys. Lett. 26B, 423 (1968).
- ¹⁹P. S. Ellis and T. Engeland, Nucl. Phys. A144, 161 (1970).
- ²⁰J. Stevens, H. F. Lutz, and S. F. Eccles, Nucl. Phys. 76, 127 (1966).
- ²¹F. Resmini, R. M. Lombard, M. Pignanelli, J. L. Escudié, and A. Tarrats, Phys. Lett. 37B, 275 (1971).
- ²²T. Hamada and I. Johnston, Nucl. Phys. 34, 382 (1962).
- ²³G. R. Satchler, Phys. Lett. 35B, 279 (1971).
- ²⁴A. P. Zuker, Phys. Rev. Lett. 23, 983 (1969).
- ²⁵R. M. Craig, *et al.*, Nucl. Instrum. Methods 30, 269 (1964).
- ²⁶H. Sherif, Ph.D. thesis, University of Washington, 1968 (unpublished).
- ²⁷A. G. Blair, C. Glashauser, R. de Swiniarski, J. Goudergues, R. Lombard, B. Mayer, J. Thirion, and P. Vaganov, Phys. Rev. C 1, 444 (1970).
- ²⁸J. L. Groh, A. P. Singhal, H. S. Caplan, and B. S. Dolbilkin, Can. J. Phys. 49, 2743 (1971).
- ²⁹R. Schaeffer, Commissariat à l'Energie Atomique Report No. R-4000 (1970).
- ³⁰J. Raynal, Nucl. Phys. A97, 572 (1967).
- ³¹T. T. S. Kuo and G. E. Brown, Nucl. Phys. 85, 40 (1966).
- ³²B. L. Scott and S. A. Moszkowski, Ann. Phys. (N. Y.) 14, 107 (1961); Nucl. Phys. 29, 655 (1962).
- ³³C. N. Bressel, A. K. Kerman, and B. Rouben, Nucl. Phys. A124, 624 (1969).
- ³⁴Y. Terrien, La Toussuire Meeting Report, 1973 (unpublished); Y. Terrien, J. L. Escudié, M. Buenerd, J. M. Loiseaux, P. Martin, J. B. Viano, Phys. Lett. 45B, 235 (1973).
- ³⁵R. Schaeffer, Nucl. Phys. A135, 231 (1969).
- ³⁶P. Federman and I. Talmi, Phys. Lett. 19, 490 (1965).
- ³⁷R. Moreh and T. Daniels, Nucl. Phys. 74, 403 (1965).
- ³⁸H. F. Lutz and S. F. Eccles, Nucl. Phys. 81, 423 (1966).
- ³⁹P. V. Hewka, R. Middleton, and J. L. Wiza, Phys. Lett. 10, 93 (1964).
- ⁴⁰R. W. Ollerhead, J. S. Lopes, A. R. Poletti, M. F. Thomas, and E. K. Warburton, Nucl. Phys. 66, 161 (1965).
- ⁴¹G. L. Morgan, D. R. Tilley, G. E. Mitchell, R. A. Hilko, and N. R. Roberson, Phys. Lett. 32B, 353 (1970).
- ⁴²G. L. Morgan, D. R. Tilley, G. E. Mitchell, R. A.

- Hilko, and N. R. Roberson, Nucl. Phys. A148, 480 (1970).
- ⁴³R. Middleton and D. J. Pullen, Nucl. Phys. 51, 63 (1964).
- ⁴⁴H. E. Gove and A. E. Litherland, Phys. Rev. 113, 1070 (1959).
- ⁴⁵F. D. Lee, R. W. Krone, and F. W. Prosser, Nucl. Phys. A96, 209 (1967).
- ⁴⁶S. Shlomo and R. Moreh, Nucl. Phys. A110, 204 (1968).
- ⁴⁷J. L. Wiza, R. Middleton, and P. V. Hewka, Phys. Rev. 141, 975 (1966).
- ⁴⁸M. Harvey, Phys. Lett. 3, 209 (1963).
- ⁴⁹B. Zeidman and T. H. Braid, Phys. Lett. 16, 139 (1965).
- ⁵⁰S. Hinds, H. Marchant, and R. Middleton, Nucl. Phys. 38, 81 (1962).
- ⁵¹A. Springer and B. G. Harvey, Phys. Rev. Lett. 14, 316 (1965).
- ⁵²R. W. Ollerhead, G. F. R. Allen, A. M. Baxter, and J. A. Kuehner, Can. J. Phys. 49, 2589 (1971).
- ⁵³Y. Terrien, Nucl. Phys. A199, 65 (1973).
- ⁵⁴D. Larson, S. M. Austin, and B. H. Wildenthal, Phys. Lett. 42B, 153 (1972).
- ⁵⁵M. Soyeur, La Toussuire Meeting Report, 1973 (unpublished); M. Soyeur and A. P. Zuker, Phys. Lett. 41B, 135 (1972).
- ⁵⁶M. Pignanelli, J. Gosset, F. Resmini, B. Mayer, and J. L. Escudié, Phys. Rev. C 8, 2120 (1973).
- ⁵⁷H. O. Benson and B. H. Flowers, Nucl. Phys. A126, 332 (1969).
- ⁵⁸B. H. Flowers and L. D. Skouras, Nucl. Phys. A136, 353 (1969).